



Why the lower stratosphere cools when the troposphere warms

Jonathan Lin^{a,b,1} and Kerry Emanuel^{c,1}

Contributed by Kerry Emanuel; received November 2, 2023; accepted January 22, 2024; reviewed by Qiang Fu and William Randel

Observational data have long suggested that in the tropics, when the troposphere locally warms, the lower stratosphere locally cools. Here, the observed anti-correlation between tropospheric and lower stratospheric temperature is confirmed—the lower stratosphere cools by approximately 2 degrees per degree of warming in the mid-troposphere. This anti-correlation is explained through a recently proposed theory holding that there is a quasi-balanced response of the stratosphere to tropospheric heating [J. Lin, K. Emanuel, Tropospheric thermal forcing of the stratosphere through quasi-balanced dynamics. *J. Atmos. Sci.* (2024).]. The local-scale anti-correlation between tropospheric and lower stratospheric temperature also holds when considering climate change—where the troposphere has been anomalously warming relative to the zonal mean, the lower stratosphere has been anomalously cooling, and vice versa. This suggests that zonally asymmetric trends in tropospheric temperature trends will be reflected in that of the lower stratospheric temperature trends. The zonally asymmetric trends are also found to be comparable in magnitude to the mean temperature trends in the lower stratosphere, highlighting the importance of the pattern of warming. The results and proposed theory suggest that in addition to forcing via wave-dissipation, the lower stratosphere can also be subject to direct forcing by the troposphere, through quasi-steady, quasi-balanced dynamics.

stratosphere | quasi-balanced dynamics | stratospheric dynamics

There is an oft-observed anti-correlation between tropospheric and lower stratospheric temperature. More specifically, when the troposphere warms, the region near and above the cold point tropopause cools; this region is henceforth referred to as the lower stratosphere. Observational studies have documented this anti-correlation on multiple time scales, from daily (1), to monthly (2, 3), to even decadal time scales (4). In the tropics, this relationship is important since the concentration of water vapor in the lower stratosphere is predominantly controlled by the dehydration process at the cold-point tropopause, on both annual (5) and interannual time scales (6–8). Since water vapor is a potent greenhouse gas, fluctuations in the stratospheric water vapor concentration have been linked to changes in global-mean surface temperature (9).

The zonally averaged temperature in the lower stratosphere has been understood as being controlled by the dissipation of waves in the tropical and sub-tropical regions (10–17). These ideas are generally derived from the theory of “downward-control,” which stipulates that, in the zonal-average, the residual vertical velocity at a given level is entirely determined by the momentum flux above that particular level (18). In the lower stratosphere, the momentum flux is thought to be provided by the dissipation of upward propagating waves. In turn, the vertical velocity determines the temperature—adiabatic cooling via upward motion must be maintained through radiative heating (of a cold anomaly). These theories, however, are based upon the transformed-Eulerian-mean (TEM) equations, which, by definition, relate the zonal-mean flow to the effect of eddies. Thus, they are only able to explain the fluctuations of the zonal mean temperature.

Using observations, we confirm that there is considerable zonal asymmetry in the temperature of the lower stratosphere. But, we also provide evidence that across a variety of time scales, including that of climate change, the spatial pattern of tropospheric temperature is mirrored in the temperature of the lower stratosphere. The data are interpreted through a simple theory that posits that there is a quasi-balanced response of the stratosphere to tropospheric heating.

Observed Anti-Correlation. We first provide evidence that confirms that local tropospheric temperature is remarkably anti-correlated with local stratospheric temperature. We use radio-occultation measurements provided by both Constellation Observing System for Meteorology Ionosphere and Climate (COSMIC) missions (COSMIC-1 and COSMIC-2). Fig. 1 shows maps of both the climatological temperature and the temperature anomaly calculated by removing the zonal mean, at 6 km, and 17 km,

Significance

Understanding the processes that control the temperature of the tropical lower stratosphere is important, since this temperature dictates the concentration of stratospheric water vapor, a potent greenhouse gas. Observational data have long shown that locally, tropospheric warming is associated with stratospheric cooling. We confirm that the temperature pattern in the troposphere is remarkably reflected in that of the lower stratosphere, and additionally show that this relationship holds when considering trends caused by climate change. We show that there is a tight coupling between the spatial pattern of tropospheric warming and stratospheric cooling. Our findings are interpreted using a simple theory that posits that there is a quasi-balanced response of the stratosphere to heating in the troposphere.

Author affiliations: ^aLamont-Doherty Earth Observatory, Columbia University, New York, NY 10027; ^bDepartment of Earth and Atmospheric Sciences, Cornell University, Ithaca, NY 14853; and ^cDepartment of Earth, Atmospheric, and Planetary Sciences, Lorenz Center, Massachusetts Institute of Technology, Cambridge, MA 02139

Author contributions: J.L. and K.E. designed research; J.L. performed research; J.L. analyzed data; and J.L. and K.E. wrote the paper.

Reviewers: Q.F., U Washington; and W.R., National Center for Atmospheric Research.

The authors declare no competing interest.

Copyright © 2024 the Author(s). Published by PNAS. This open access article is distributed under Creative Commons Attribution-NonCommercial-NoDerivatives License 4.0 (CC BY-NC-ND).

¹To whom correspondence may be addressed. Email: jonathanlin@cornell.edu or emanuel@mit.edu.

This article contains supporting information online at <https://www.pnas.org/lookup/suppl/doi:10.1073/pnas.2319228121/-DCSupplemental>.

Published March 4, 2024.

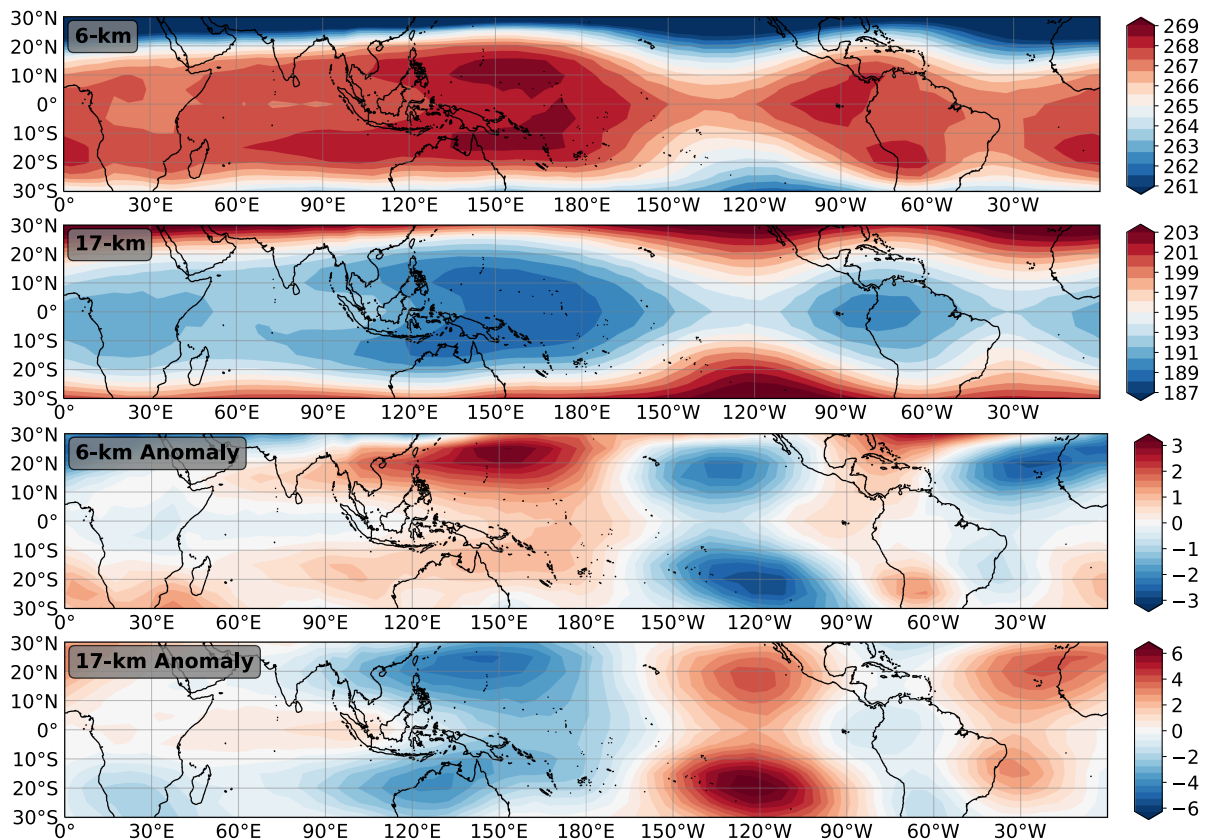


Fig. 1. (Top): Map of the climatological DJF temperature at 6 km (K). (Middle-Top): Same as top but at 17 km. (Middle-Bottom): Map of the DJF temperature at 6 km, but with the climatological zonal mean in DJF removed. (Bottom): Same as Middle-Bottom, but at 17 km. Note the color scale at 17 km is twice that at 6 km.

during the boreal winter season (DJF). These levels are chosen to broadly represent the mid-troposphere and lower stratosphere. There is an astounding anti-correlation between tropospheric temperature and the lower-stratospheric temperature, both in the climatology ($r = -0.88$), and in anomalies from the zonal mean ($r = -0.76$). In other words, the spatial heating patterns at 6 km strongly imprint on that at 17 km. Linear fits between the grid-point temperature anomaly at 6 km and that at 17 km, from 30°S to 30°N, show that per degree of warming at 6 km, there is around 1.6° of cooling at 17 km. Similar calculations were performed across varying seasons, since there is a seasonality in tropospheric heating. The relationships are robust, though correlations are highest in DJF and lowest in boreal summer (SI Appendix, Figs. S1–S3).

To understand the vertical dependence of the observed anti-correlation, we perform the same grid-point correlations, but co-vary the vertical levels at which the temperature anomalies are correlated. In other words, across all grid points, we correlate the temperature anomaly at a base level x with that at level y , as shown in Fig. 2A. The same analysis, except using the climatological temperature, is nearly identical to that shown in Fig. 2 (SI Appendix, Fig. S4). Immediately obvious is that a column of the troposphere heats almost entirely in unity (up until around 14 km). The magnitude of the column approximately follows a moist adiabat—per degree of warming in the lower troposphere, there is greater warming in the mid and upper troposphere, as shown in Fig. 2B. In general, the correlations with upper tropospheric temperature decrease as one moves downward, closer to the boundary layer. This is unsurprising, as inversion layers can often form in the tropics when the boundary

layer moist static energy is smaller than the saturation moist static energy of the free troposphere. This generally occurs over regions of relatively colder sea surface temperature.

Most strikingly, Fig. 2 shows that the local temperature in the lower stratosphere can be predicted if one knows the local tropospheric temperature. Tropospheric-only models of moist convection stay silent on the temperature and geopotential response above the level of neutral buoyancy. But, Fig. 2 shows that the cooling in the lower stratosphere, in association with tropospheric warming, can be quite large: around 2 times larger than that of the 4 km temperature anomaly. The upward temperature response decays quite rapidly higher into the stratosphere, to around -0.5° in magnitude at around 20 km. Note that the height-dependent correlations are performed from 20°S to 20°N. The magnitude of the tropospheric correlations is slightly smaller when extending to 30°S to 30°N, but still large and significant (SI Appendix, Fig. S5).

Stratospheric Response to Tropospheric Forcing. The remarkable connection between tropospheric temperature and lower stratospheric temperature is deserving of a physical explanation. To our knowledge, there is only one explicit explanation for the ubiquitous anti-correlation between tropospheric and lower stratospheric temperature on local scales—that of a “convective cold top” (1). This theory posits that above regions of tropospheric warming, there is an adjustment to hydrostatic balance, which enforces that the pressure gradients decay with height, thus generating a cold anomaly. Crucial to this argument is the assumption of a fixed level at which the pressure gradient vanishes. The adjustment to hydrostatic balance must occur on

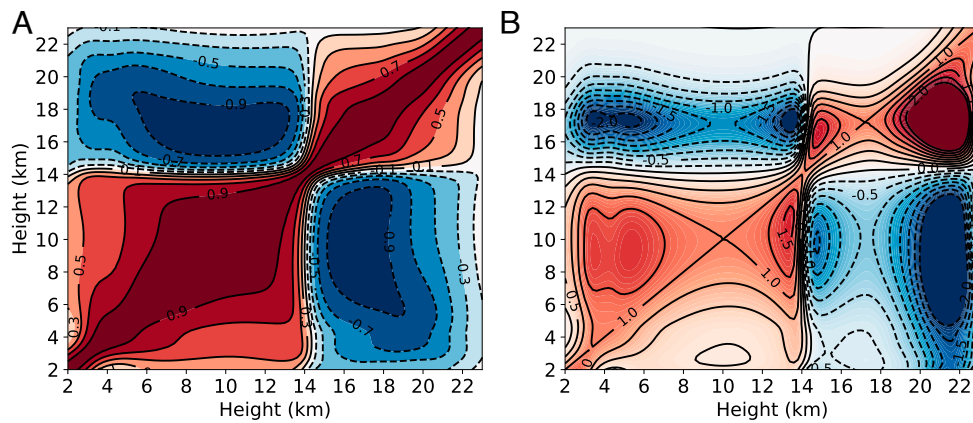


Fig. 2. (A): Pearson correlations of the linear fit between temperature anomalies at the vertical level denoted by the ordinate axis, per degree of warming at the level denoted by the abscissa axis. Contour spacing is 0.2, and data is calculated using the DJF climatology, from -20°S to 20°N . (B): Same as (A), but showing the magnitude of the temperature anomaly at the level denoted by the ordinate axis. Contour spacing is 0.25. Local stratospheric cooling is strongly correlated with local tropospheric warming.

extremely fast time scales and was estimated to occur on the order of half an hour (1). Furthermore, the theory lacks a scaling for the magnitude of the temperature anomalies in the stratosphere, with respect to the temperature anomalies in the troposphere.

Alternatively, a recently proposed theory by the authors suggests that there is a quasi-steady, quasi-balanced response of the stratosphere to tropospheric heating (20). To qualitatively understand the physical mechanism, we first consider a troposphere in radiative-convective equilibrium, with an overlying stratosphere at rest. Suppose that the troposphere is forced through the imposition of a warm sea surface temperature anomaly. The troposphere warms, following a moist adiabat, the pressure at the surface falls, and the geopotential rises at the tropopause. Since pressure cannot be discontinuous across the tropopause, there must be a response in the stratosphere. The geopotential anomaly initially decays with increasing height in the stratosphere, according to a height scale that follows the Rossby penetration depth, $R_d = f_0 L / N$, where f_0 is the Coriolis force, L is the horizontal length scale of the anomaly, and N is the buoyancy frequency. Note that in the tropics, R_d is very small. This process occurs on the time scale of geostrophic adjustment.

Since the geopotential anomaly decays with height, a cold anomaly must be initially present above the tropopause. Thereafter, rising motion accompanies the cold anomaly, since the associated radiative heating must be balanced by adiabatic cooling. Over a long period of time, the cold anomaly migrates upward in the stratosphere as it is radiatively heated. Thus, despite the smallness of R_d in the tropics, radiative adjustment acts to make the cold anomaly “taller” and weaker. This process occurs slowly, however, since in the tropical lower stratosphere, the radiative relaxation time scale is approximately a month (19). Regardless, the theory predicts the presence of a local cold anomaly above a local warm anomaly and serves as an alternative explanation of the oft-observed anti-correlation between tropospheric and lower stratospheric temperature.

The proposed theory argues that the stratosphere is thermally forced by the troposphere through quasi-steady, quasi-balanced dynamics. It matters not whether the thermal forcing is provided through heating of the ocean, or more generally through large-scale tropospheric heating. As a mathematical shortcut, one can think about the stratosphere being thermally forced by the troposphere through the imposition of a geopotential anomaly at the tropopause (in reality, the tropopause geopotential is also influenced by the stratosphere itself). In this way, the theory

can be easily generalized to regions where there is less of a direct coupling to the ocean—such as over land, and in the subtropics/extratropics. Furthermore, this perspective means that any disturbance that has an upper-tropospheric geopotential anomaly can elicit a quasi-balanced response in the stratosphere. This is including, but not limited to, monsoons, the Tibetan anticyclone, mesoscale convective systems, and tropical cyclones.

A third explanation, involving the vertical propagation of quasi-stationary waves, could also potentially explain features of the observational data, though it has only been used to explain the anti-correlation in zonally asymmetric tropospheric and lower stratospheric temperature (and not the climatology) (12, 21, 22). This mechanism is especially attractive, since the Eliassen-Palm (EP) flux divergence associated with the quasi-stationary waves can connect with wave-driving theories. Tropical and sub-tropical stationary waves excited as a response to tropical heating tend to have baroclinic vertical structures (23), which matches the tropospheric vertical profiles of temperature shown in Fig. 2. The stratospheric component of an upward propagating quasi-stationary wave, however, does not necessarily have to possess a vertical structure that is associated with cooling in the lower stratosphere, as the characteristics and vertical propagation of the tropospherically forced stationary wave strongly depend on the background state (24, 25). However, models generally show that the vertical propagation of stationary waves in the tropics is strongly inhibited (26). The geopotential amplitude associated with the damped stationary wave decreases with increasing height in the stratosphere, implying a lower stratospheric cooling signature that also decays strongly with height, consistent with the observational data (Fig. 2).

Note, however, that there is a strong anti-correlation in tropospheric and lower stratospheric climatological temperature even close to the equator, where the Coriolis parameter is small, as indicated by Fig. 1. This behavior is not readily explained by wave-based theories. Still, it is important to highlight the subtle differences between the quasi-balanced response of the stratosphere to tropospheric heating, and the upward propagation of stationary waves that can be excited in response to heating. We return to our radiative-convective equilibrium troposphere and impose a warm sea surface temperature anomaly at the equator. In the case of a constant Coriolis force everywhere, there would be no stationary Rossby waves associated with the heating. However, a cold anomaly would still form above the tropopause, since pressure cannot be discontinuous across the tropopause. In

contrast, suppose there are gradients in the Coriolis force. In the simplest case where there is no background wind anywhere, a Gill-like pattern appears in the troposphere as a response to a stationary SST anomaly at the equator (27). While the quasi-balanced stratospheric response would be to cool, an important question is whether the steady stratospheric response can “survive” given the possibility of equatorial Rossby waves. The behavior of these waves will depend strongly on the background zonal wind in the stratosphere. Owing to these nuances, we cannot, at present, explicitly rule out the role of the vertical propagation of stationary waves. It is likely that both mechanisms play a role in modulating lower stratospheric temperature in the real world.

Time Scale Dependence. In the previous section, we analyzed the anti-correlation between tropospheric and lower stratospheric temperature on climatological time scales. To what extent does the relationship hold on faster time scales? We answer this question by performing linear correlations between the grid-point temperature anomalies at 8 km and 17 km, using varying time-averaging periods. Given the high correlations with lower stratospheric temperature, 8 km is chosen as representative of mid-tropospheric temperature (Fig. 2). Fig. 3 shows that on daily, monthly, seasonal, and interannual time scales, the asymmetric pattern of 8-km temperature imprints itself onto the pattern of 17-km temperature. The anti-correlations are robust and significant even during relatively fast time scales (i.e., 3 d). Across the observed time period, the average correlation is $r = -0.70$ for the 3-d time scale, $r = -0.73$ for the weekly time scale, $r = -0.82$ for the monthly time scale, $r = -0.87$ for the seasonal time scale, and $r = -0.96$ for the annual time scale. Thus, the extent to which tropospheric temperature influences temperature in the lower stratosphere is mediated by the time scale: The longer the time scale, the stronger the influence.

To what extent could the observed anti-correlation reflect the vertical propagation of convectively-coupled equatorial waves or gravity waves? These waves generally propagate along the equator and upward into the stratosphere, with periods from a few days to longer than a month. They have a phase tilt in the stratosphere that is proportional to their horizontal phase speed (and their horizontal scale) (28). Because of this phase tilt, it is not necessary that the 17-km temperature, or the whole lower stratosphere for that matter, be anti-correlated with tropospheric temperature. A wave with just the right vertical wavenumber would need to dominate the wave spectrum in order for the entire lower stratosphere to be anti-correlated with tropospheric

temperature. Wave number-frequency decompositions show a red-noise background spectrum in both the tropical troposphere (29) and lower stratosphere (30), such that it is unlikely that the upward propagation of equatorial waves or gravity waves can explain this phenomenon. This suggests that increasing the time-averaging window smooths out both sampling error and temperature variability from upward propagating waves.

Historical Trends. In the previous two sections, we showed that the local temperature in the lower stratosphere can be well predicted by the local tropospheric temperature. A natural follow-up is to ask whether or not this relationship extends to climate-change time scales. To answer this, we compute linear trends of temperature over 1979 to 2022, using ERA5 reanalysis. In order to emphasize the spatial variability of the temperature trends, we subtract out the zonally averaged trend at each latitude (*SI Appendix, Fig. S7* shows the raw trends). Fig. 4 shows the anomalous trend of temperature at the sea-surface, 500 hPa, the cold-point tropopause, and 70 hPa. We observe that the anomalous trends at 500 hPa broadly resemble a Gill-like response to a stationary heating at the equator (27). Strikingly, the patterns of anomalous temperature trend at the cold-point tropopause and 70 hPa are nearly mirror (opposite in sign) that at 500 hPa. In other words, where the free troposphere is anomalously cooling, the lower stratosphere is anomalously warming, and vice versa. The trend patterns at 500 hPa and the cold-point resemble temperature patterns that are related to El Niña-like variability (31) and could thus be related to the observed increase in zonal sea-surface temperature (SST) gradient near the equator (or a trend toward a more “La Niña-like” state) (32).

We can quantitatively analyze the anti-correlation between tropospheric temperature trends and lower stratospheric temperature trends by repeating the analysis shown in Fig. 2. Fig. 5 shows that even on climate change time scales, the local temperature trend in the mid-troposphere can skillfully predict the local temperature trend in the lower stratosphere. We note the striking similarity between Figs. 2 and 5 (though the two are not exactly the same since the former is evaluated in height coordinates and during DJF, and the latter in pressure coordinates). In general, warming between 850 and 600 hPa is less correlated with temperature changes aloft, as compared to climatology (c.f. Figs. 2 and 5). This behavior is mostly an effect of annual averaging and also observed in the climatological data

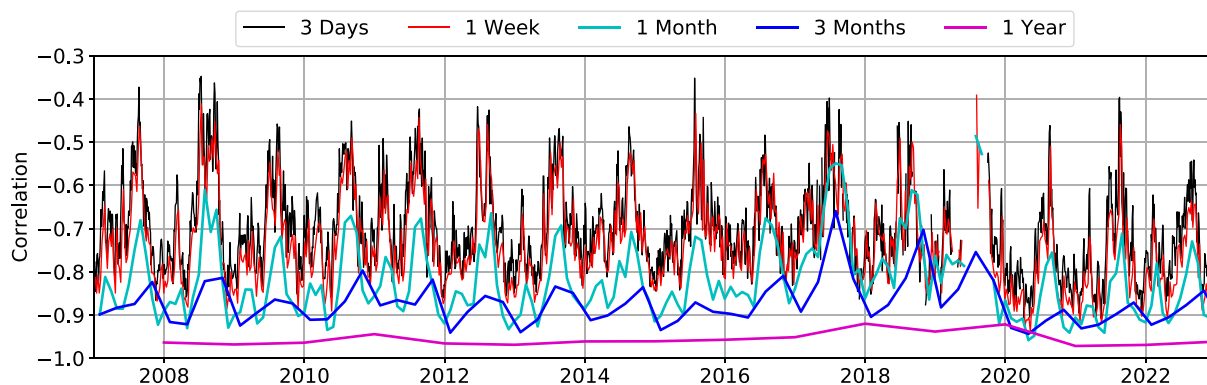


Fig. 3. Correlations of the linear fit between grid-point 8 km temperature anomalies from the climatological zonal monthly mean, and those at 17 km, with varying time-averaging periods. Line colors indicate time averaging period. Correlations are performed over the region 20°S to 20°N. Only data points with a minimum of at least 100 passes over the region and time period are shown.

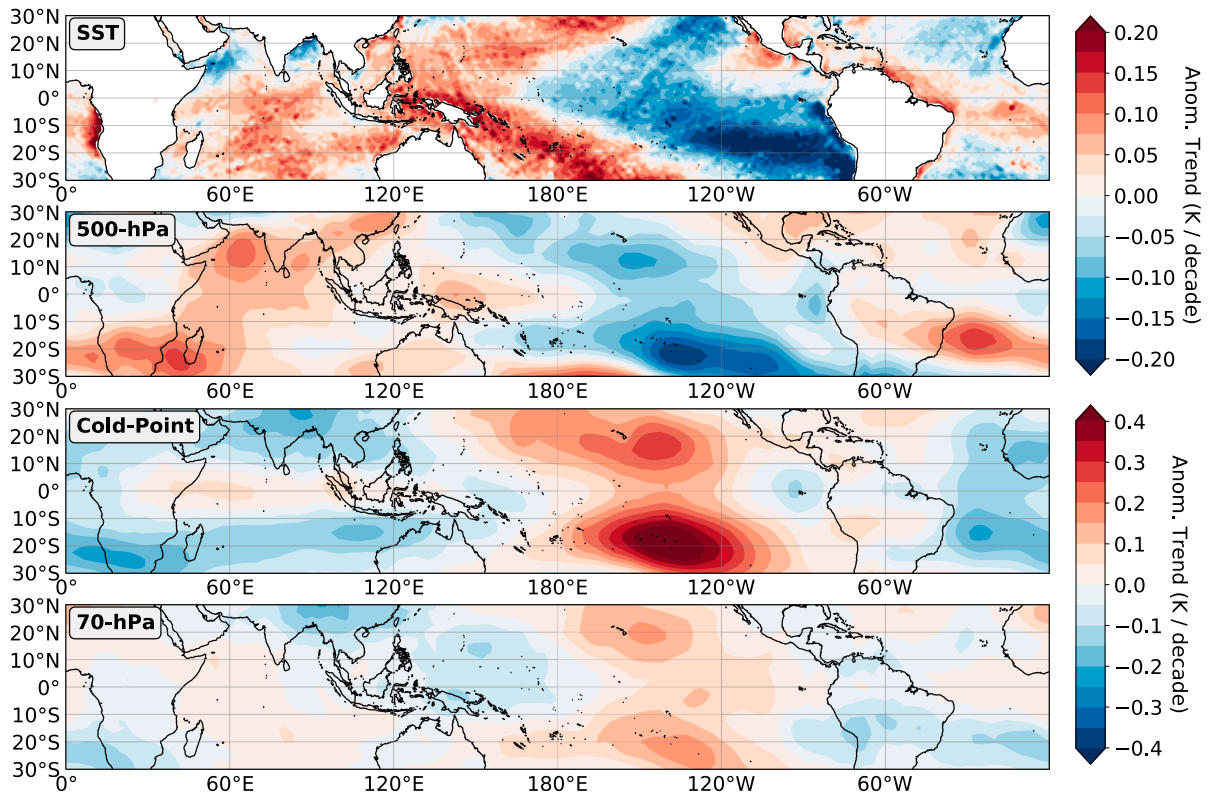


Fig. 4. Anomalous linear trends in temperature at the sea-surface, 500 hPa, cold-point, and 70 hPa, in the ERA5 reanalysis, from 1979 to 2022. Anomalies in trends are computed with respect to the zonally averaged linear trend and shown in K per decade. Note the color scale of the *Bottom* two panels is two times that of the first two panels.

when calculating correlations over annual-averaged anomalies (*SI Appendix, Fig. S6*).

The sign of the temperature response to tropospheric warming switches from positive to negative at around 175 hPa. The local cooling response to tropospheric warming maximizes slightly above 100 hPa and decays with decreasing pressure into the stratosphere. Note, the annual-mean tropical cold-point tropopause is also slightly above 100 hPa (33). Per degree of local warming trend at 500 hPa, there is around a 1.7° of a local cooling trend at 100 hPa, decaying in magnitude as one moves upward in the stratosphere.

These results provide strong evidence that the anti-correlation between tropospheric and lower stratospheric temperature also exists on climate change time scales. However, it is also important to note that in response to tropospheric warming, there is cooling from approximately 150 to 100 hPa, below the annual-mean tropical cold-point tropopause (33). The recently proposed theory does not explicitly take into account the tropical tropopause layer (TTL), the transition region between the troposphere and stratosphere (34). As such, cooling below the cold-point tropopause in response to tropospheric warming is not readily explained by the proposed theory of Lin and Emanuel (20).

Up until now, we have only shown that anomalous tropospheric temperature trends can predict anomalous lower stratospheric trends. While it is immediately clear why mean trends are important, the same cannot be said for anomalous trends. The pattern of the anomalous warming/cooling trends far from the surface is only important to understand if it 1) is of comparable magnitude to the mean trend, and/or 2) is a factor in Earth's equilibrium climate sensitivity. Research has shown that the water vapor flux into the stratosphere is predominantly

controlled by the Lagrangian cold-point tropopause temperature (7). As such, the spatial pattern of cold-point tropopause trends may be important for the water vapor flux into the stratosphere, especially if the cold-point tropopause temperature changes over regions where there is a large degree of tropospheric transport of water vapor into the stratosphere. However, future changes to the Lagrangian cold-point tropopause temperature will also depend on the three-dimensional circulation response to warming, not just the temperature pattern trends. As a result, further research is required before making conclusions on the second point. For now, we provide evidence for the first point.

To illustrate this, Fig. 6, solid-black line, shows vertical profiles of the tropically averaged (20°S to 20°N) temperature trend, calculated over 1979 to 2022, using ERA5 reanalysis. Linear regression of the anomalous temperature trend at 500 hPa, with that at other vertical levels, is shown in Fig. 6, red. Broadly, there is greater mean warming in the upper troposphere than the lower troposphere, and strong stratospheric cooling, a large portion of which has been attributed to the destruction of ozone (35–37).

We next compute the average magnitude of the temperature trend deviation from the zonal-mean trend, henceforth referred to as the magnitude of the anomalous trend, which acts as a proxy for the zonal asymmetry in warming/cooling. The magnitude of the anomalous trend is shown in Fig. 6, dashed-black. In the troposphere, there is a significant amount of mean warming, such that the magnitude of the anomalous trends is approximately a third that of the mean trend. There is a minimum in the magnitude of the anomalous trend at 175 hPa associated with the sign reversal of the temperature response to tropospheric warming. Above 175 hPa, there is strong cooling associated with warming at 500 hPa, with both the magnitude of the

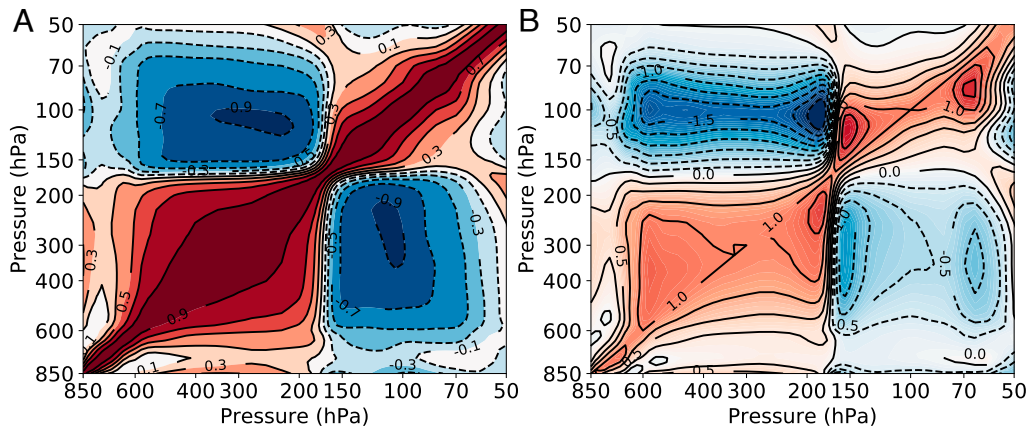


Fig. 5. (A): Pearson correlations of the linear fit between anomalous temperature trends at the pressure level denoted by the ordinate axis, and the anomalous temperature trend at the pressure level denoted by the abscissa axis. Contour spacing is 0.2, and data are calculated using the ERA5 linear trends from 1979 to 2022, over -30°S to 30°N . (B): Same as (A), but showing the magnitude of the linear fit. Contour spacing is 0.25.

cooling response and the magnitude of zonal asymmetry rapidly increasing with decreasing pressure, peaking at ≈ 100 hPa. Most importantly, at both the cold-point tropopause, and more broadly in a small layer from approximately 125 to 90 hPa, the magnitude of the anomalous trends is more than half that of the mean-trend, as shown by the shaded region in Fig. 6. This is because in this region, the mean temperature trend shifts from warming to cooling, while the magnitude of the anomalous trends maximizes. Finally, the magnitude of the anomalous trends decreases with decreasing pressure further into the stratosphere; correspondingly, the magnitude of the temperature response to tropospheric warming also decreases.

It is perhaps unsurprising that the mean trend near the tropopause is close to zero. Tropospheric warming and stratospheric cooling can largely cancel out in this region, which, in addition to data sparsity and quality-control issues, leads to large uncertainties in the temperature response to anthropogenic forcing (38, 39), especially across various observational and reanalyses products (40). Thus, temperature trends near the tropopause should be interpreted with caution. Regardless, the results show that the anomalous trend may be just as important as the mean trend in the lower stratosphere, which may have implications for future changes to the water vapor flux into the stratosphere.

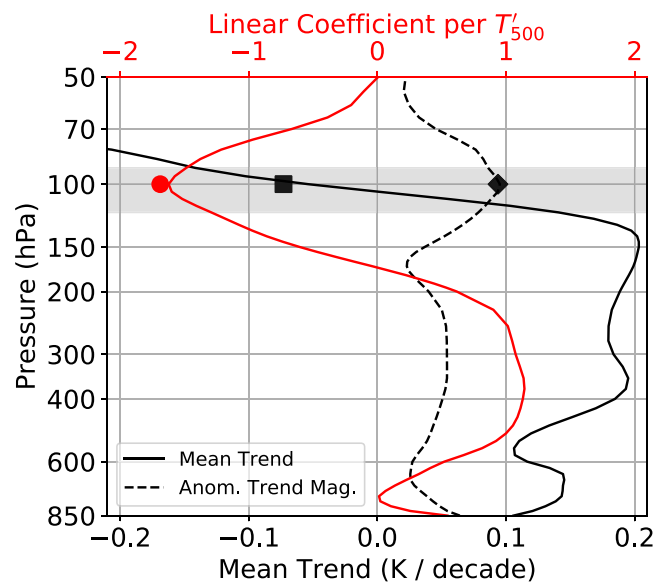


Fig. 6. The solid-black line shows the tropically averaged (20°S to 20°N) trend in temperature (K per decade) at varying pressure levels. Trends are calculated over 1979 to 2022 using ERA5 reanalysis data. The dashed-black line shows the average magnitude of the deviation from the zonal-mean temperature trend (i.e., magnitude of the anomalous trends) over the same period/region. The shaded gray region indicates levels where the magnitude of the anomalous trends exceeds half the magnitude of the mean trend. The red solid line shows the linear coefficient of the anomalous temperature trend at varying vertical levels regressed onto the anomalous temperature trend at 500 hPa. The shaded square, diamond, and circle are, respectively, the mean trend, anomalous trend magnitude, and linear coefficient, except evaluated at the cold-point tropopause.

Summary and Discussion. In this work, we provide a potential explanation for the ubiquitous anti-correlation between tropospheric temperature and lower stratospheric temperature. Since a warming of the troposphere is associated with decreasing surface pressure and a positive geopotential anomaly at the tropopause, the stratosphere must respond, as pressure cannot be discontinuous across the tropopause. The geopotential anomaly initially decreases with increasing height, and the associated cold anomaly is balanced by radiative heating. This simple physical explanation posits that there is a quasi-balanced response of the stratosphere to large-scale tropospheric heating.

Analysis of observational data taken from 15 y of GPS radio-occultation measurements shows that on a variety of time scales, the troposphere is remarkably anti-correlated with lower stratospheric temperature. The correlations occur on the local-scale, in both the climatological base state, as well as in anomalies calculated by removing the zonal mean (Fig. 1). The lower stratosphere cools by nearly 2° per degree of heating at 6 km. Correlations performed over varying time scales also show that the strength of tropospheric influence on lower stratospheric temperature increases as the time scale is increased, from $r = -0.70$ at a 3-d time scale, to $r = -0.96$ at an annual time scale. The troposphere thus exerts a strong influence on lower stratospheric temperature across a variety of time scales. It is hypothesized that upward propagating higher frequency waves can disrupt the observed anti-correlations, though further analysis by regressing out high-frequency variability could be performed in future work.

We also analyze historical trends in temperature and find that on climate-change time scales, the local temperature trend in the troposphere is also strongly anti-correlated with that in the lower

stratosphere. We show that the local cooling/warming patterns are of comparable magnitude to the mean trends in the lower stratosphere, owing both to the smallness of mean trends and a maximization of the anti-correlation signal near the cold-point tropopause. Our results imply that the pattern of tropospheric warming will strongly influence the pattern of temperature trends in the lower stratosphere.

The connection between tropospheric warming and stratospheric cooling is not a new idea. In fact, there is already much literature that connects tropical-averaged SST with the Brewer–Dobson mass flux. In both models and re-analyses, there are strong correlations between the tropically averaged SST and the 70-hPa mass flux (41–44). For example, interannual variability in tropically averaged SST explains around half of the interannual variability in the vertical mass flux at 70 hPa (42, 44). These strong correlations between tropically averaged SST and lower stratospheric mass flux have been explained through the theory of downward-control: Warming in the tropics warms the upper troposphere, which alters the sub-tropical jets and increases the wave-dissipation in the sub-tropics (42, 45, 46). However, as this work emphasizes, there is a large degree of zonally asymmetric variability in the temperature near the tropopause that seems to mostly be a consequence of zonally asymmetric patterns in tropospheric temperature (47). This zonally asymmetric variability is not well explained by existing wave-driving theories, which can only explain variations in the zonally averaged temperature.

This work may have implications for our understanding of the stratospheric water vapor feedback. Most CMIP6 models show that the cold-point tropopause warms with increasing greenhouse gas emissions, increasing the stratospheric water vapor concentration (48)—in other words, the zonal-mean tropospheric temperature is positively correlated with the mean cold-point tropopause temperature. In contrast, our work emphasizes the negative correlation between the two, but on local scales. The sign difference in the relationship of tropopause temperature with tropospheric temperature perhaps arises because of 1) a systematic deficiency in CMIP6 models (for instance, inadequate vertical resolution near the tropopause), or 2) a difference in the mechanisms that are responsible for changes in cold-point tropopause temperature on the zonal-mean scale vs. the local-scale (47).

Regardless, we believe that the pattern of temperature trends in the lower stratosphere may be important in determining the stratospheric water vapor feedback, though this will also depend on the 3-dimensional circulation response to warming. In general, the upward diabatic mass flux of water vapor is proportional to the amplitude of the cold anomaly in the lower stratosphere. Thus, the colder the temperature anomaly, the drier the air being moved into the lower stratosphere. This simple relation implies

that merely increasing the variance of tropopause temperature will serve to dry out the stratosphere. Since the observed anti-correlation between local tropospheric and lower stratospheric temperature also holds on climate-change time scales, it will be important to understand how the pattern of tropospheric temperature might change as a consequence of anthropogenic greenhouse emissions.

Materials and Methods

GPS Radio-Occultation Data. We use data from the COSMIC-1 (2007-2019) and COSMIC-2 (2019-present) missions, available at <https://data.cosmic.ucar.edu/gnss-ro/cosmic1/repro2021/level2/> (52) and <https://data.cosmic.ucar.edu/gnss-ro/cosmic2/nrt/level2/> (53), respectively. The mission publishes Level 2 “wetPf2” files, which are radio-occultation profiles in which gridded analyses or short-term forecasts are used to separate the contributions of pressure, temperature, and moisture to refractivity. The profiles have an interpolated vertical resolution of 100 m. We aggregate the occultation profiles with a spatial resolution of 5° longitude by 5° latitude, and a temporal resolution of 1 d. Furthermore, we truncate the radio-occultation profiles at 2 km and below, due to super-refraction that can often occur in the tropical and sub-tropical boundary layers with sharp inversions (49).

In Fig. 3, the specified time-averaging window dictates the temporal resolution over which the occultation profiles are aggregated. For instance, when the time-averaging window is 1 wk, all profiles over a 1-wk window are averaged together to determine the grid-box average. A linear regression is then fit to the scatter among all grid boxes to determine the correlation. We require a minimum of 100 passes over the tropical region during the specified time window, for robustness. Thus, there are breaks in observational data in the second half of 2019, as COSMIC-1 was decommissioned and COSMIC-2 was launched.

ERA5 Reanalysis Data. We use monthly averaged temperature data from the complete ERA5 reanalysis, over the periods 1979 to 2022. Over the periods 1979 to 1999, and 2007 to 2022, we use the complete ERA5 reanalysis (50) via DOI: [10.24381/cds.143582cf](https://doi.org/10.24381/cds.143582cf), and over the period 2000 to 2006, we use the complete ERA5.1 reanalysis (51) via <https://doi.org/10.24381/cds.143582cf>. The ERA5 reanalysis data are accessible by creating an account with the Climate Data Store service, and usable according to ECMWF license to use Copernicus products. The complete ERA5 data are provided on 138 model levels, which have high vertical resolution in the lower stratosphere. The model levels are interpolated to pressure levels, with a spacing in pressure coordinates of 25 hPa from 850 to 250 hPa, and 5 hPa from 250 to 50 hPa.

Data, Materials, and Software Availability. Previously published data were used for this work (<https://data.cosmic.ucar.edu/gnss-ro/cosmic1/repro2021/level2/> (52), and <https://data.cosmic.ucar.edu/gnss-ro/cosmic2/nrt/level2/> (53)).

ACKNOWLEDGMENTS. J.L. gratefully acknowledges the support of the NSF through the NSF-AGS Postdoctoral Fellowship, under award number AGS-PRF-2201441.

1. C. E. Holloway, J. D. Neelin, The convective cold top and quasi equilibrium. *J. Atmos. Sci.* **64**, 1467–1487 (2007).
2. A. Gettelman, M. L. Salby, F. Sassi, Distribution and influence of convection in the tropical tropopause region. *J. Geophys. Res. Atmos.* **107**, ACL-6 (2002).
3. J. Kim, W. J. Randel, T. Birner, Convectively driven tropopause-level cooling and its influences on stratospheric moisture. *J. Geophys. Res. Atmos.* **123**, 590–606 (2018).
4. F. Qiang, C. M. Johanson, J. M. Wallace, T. Reichler, Enhanced mid-latitude tropospheric warming in satellite measurements. *Science* **312**, 1179 (2006).
5. P. W. Mote *et al.*, An atmospheric tape recorder: The imprint of tropical tropopause temperatures on stratospheric water vapor. *J. Geophys. Res. Atmos.* **101**, 3989–4006 (1996).
6. W. J. Randel, W. Fei, S. J. Oltmans, K. Rosenlof, G. E. Nedoluha, Interannual changes of stratospheric water vapor and correlations with tropical tropopause temperatures. *J. Atmos. Sci.* **61**, 2133–2148 (2004).
7. S. Fueglistaler, M. Bonazzola, P. H. Haynes, T. Peter, Stratospheric water vapor predicted from the Lagrangian temperature history of air entering the stratosphere in the tropics. *J. Geophys. Res. Atmos.* **110** (2005).
8. W. Randel, M. Park, Diagnosing observed stratospheric water vapor relationships to the cold point tropical tropopause. *J. Geophys. Res. Atmos.* **124**, 7018–7033 (2019).
9. S. Solomon *et al.*, Contributions of stratospheric water vapor to decadal changes in the rate of global warming. *Science* **327**, 1219–1223 (2010).
10. E. Yulaeva, J. R. Holton, J. M. Wallace, On the cause of the annual cycle in tropical lower-stratospheric temperatures. *J. Atmos. Sci.* **51**, 169–174 (1994).
11. J. R. Holton *et al.*, Stratosphere-troposphere exchange. *Rev. Geophys.* **33**, 403–439 (1995).
12. W. A. Norton, Tropical wave driving of the annual cycle in tropical tropopause temperatures. Part II: Model results. *J. Atmos. Sci.* **63**, 1420–1431 (2006).
13. W. J. Randel, R. Garcia, W. Fei, Dynamical balances and tropical stratospheric upwelling. *J. Atmos. Sci.* **65**, 3584–3595 (2008).
14. J.-H. Ryu, S. Lee, Effect of tropical waves on the tropical tropopause transition layer upwelling. *J. Atmos. Sci.* **67**, 3130–3148 (2010).
15. D. A. Ortland, M. J. Alexander, The residual-mean circulation in the tropical tropopause layer driven by tropical waves. *J. Atmos. Sci.* **71**, 1305–1322 (2014).

16. J. Kim, W. J. Randel, T. Birner, M. Abalos, Spectrum of wave forcing associated with the annual cycle of upwelling at the tropical tropopause. *J. Atmos. Sci.* **73**, 855–868 (2016).
17. M. Jucker, E. P. Gerber, Untangling the annual cycle of the tropical tropopause layer with an idealized moist model. *J. Clim.* **30**, 7339–7358 (2017).
18. P. H. Haynes *et al.*, On the “downward control” of extratropical diabatic circulations by eddy-induced mean zonal forces. *J. Atmos. Sci.* **48**, 651–678 (1991).
19. P. Hitchcock, T. G. Shepherd, S. Yoden, On the approximation of local and linear radiative damping in the middle atmosphere. *J. Atmos. Sci.* **67**, 2070–2085 (2010).
20. J. Lin, K. Emanuel, Tropospheric thermal forcing of the stratosphere through quasi-balanced dynamics. *J. Atmos. Sci.* (2024).
21. I. M. Dima, J. M. Wallace, Structure of the annual-mean equatorial planetary waves in the ERA-40 reanalyses. *J. Atmos. Sci.* **64**, 2862–2880 (2007).
22. K. M. Grise, D. W. J. Thompson, On the signatures of equatorial and extratropical wave forcing in tropical tropopause layer temperatures. *J. Atmos. Sci.* **70**, 1084–1102 (2013).
23. T.-C. Chen, The structure and maintenance of stationary waves in the winter northern hemisphere. *J. Atmos. Sci.* **62**, 3637–3660 (2005).
24. J. G. Charney, P. G. Drazin, Propagation of planetary-scale disturbances from the lower into the upper atmosphere. *J. Geophys. Res.* **66**, 83–109 (1961).
25. I. M. Held, Stationary and quasi-stationary eddies in the extratropical troposphere: Theory. *Large-Scale Dyn. Processes Atmos.* **127**, 168 (1983).
26. H. Gamy, M. Dameris, W. Randel, G. E. Bodeker, R. Deckert, Dynamically forced increase of tropical upwelling in the lower stratosphere. *J. Atmos. Sci.* **68**, 1214–1233 (2011).
27. A. E. Gill, Some simple solutions for heat-induced tropical circulation. *Q. J. R. Meteorol. Soc.* **106**, 447–462 (1980).
28. J. Lin, K. Emanuel, On the effect of surface friction and upward radiation of energy on equatorial waves. *J. Atmos. Sci.* **79**, 837–857 (2022).
29. M. Wheeler, G. N. Kiladis, Convectively coupled equatorial waves: Analysis of clouds and temperature in the wavenumber-frequency domain. *J. Atmos. Sci.* **56**, 374–399 (1999).
30. W. J. Randel, W. Fei, A. Podglajen, Equatorial waves, diurnal tides and small-scale thermal variability in the tropical lower stratosphere from COSMIC-2 radio occultation. *J. Geophys. Res. Atmos.* **126**, e2020JD033969 (2021).
31. E. Yulaeva, J. M. Wallace, The signature of ENSO in global temperature and precipitation fields derived from the microwave sounding unit. *J. Clim.* **7**, 1719–1736 (1994).
32. K. B. Karnauskas, R. Seager, A. Kaplan, Y. Kushnir, M. A. Cane, Observed strengthening of the zonal sea surface temperature gradient across the equatorial Pacific Ocean. *J. Clim.* **22**, 4316–4321 (2009).
33. J. Kim, S.-W. Son, Tropical cold-point tropopause: Climatology, seasonal cycle, and intraseasonal variability derived from COSMIC GPS radio occultation measurements. *J. Clim.* **25**, 5343–5360 (2012).
34. S. Fueglistaler *et al.*, Tropical tropopause layer. *Rev. Geophys.* **47** (2009).
35. P. M. Forster, G. Bodeker, R. Schofield, S. Solomon, D. Thompson, Effects of ozone cooling in the tropical lower stratosphere and upper troposphere. *Geophys. Res. Lett.* **34** (2007).
36. L. M. Polvani, S. Solomon, The signature of ozone depletion on tropical temperature trends, as revealed by their seasonal cycle in model integrations with single forcings. *J. Geophys. Res. Atmos.* **117** (2012).
37. L. M. Polvani, L. Wang, V. Aquila, D. W. Waugh, The impact of ozone-depleting substances on tropical upwelling, as revealed by the absence of lower-stratospheric cooling since the late 1990s. *J. Clim.* **30**, 2523–2534 (2017).
38. A. Gettelman *et al.*, The tropical tropopause layer 1960–2100. *Atmos. Chem. Phys.* **9**, 1621–1637 (2009).
39. J. S. Wang, D. J. Seidel, M. Free, How well do we know recent climate trends at the tropical tropopause? *J. Geophys. Res. Atmos.* **117** (2012).
40. S. Tegmeier *et al.*, Temperature and tropopause characteristics from reanalyses data in the tropical tropopause layer. *Atmos. Chem. Phys.* **20**, 753–770 (2020).
41. W. J. Randel, R. R. Garcia, N. Calvo, D. Marsh, ENSO influence on zonal mean temperature and ozone in the tropical lower stratosphere. *Geophys. Res. Lett.* **36** (2009).
42. P. Lin, Y. Ming, V. Ramaswamy, Tropical climate change control of the lower stratospheric circulation. *Geophys. Res. Lett.* **42**, 941–948 (2015).
43. C. Orbe *et al.*, GISS Model E2. 2: A climate model optimized for the middle atmosphere-2. Validation of large-scale transport and evaluation of climate response. *J. Geophys. Res. Atmos.* **125**, e2020JD033151 (2020).
44. M. Abalos *et al.*, The Brewer-Dobson circulation in CMIP6. *Atmos. Chem. Phys.* **21**, 13571–13591 (2021).
45. R. R. Garcia, W. J. Randel, Acceleration of the Brewer-Dobson circulation due to increases in greenhouse gases. *J. Atmos. Sci.* **65**, 2731–2739 (2008).
46. R. R. Natalia Calvo, W. J. R. Garcia, D. R. Marsh, Dynamical mechanism for the increase in tropical upwelling in the lowermost tropical stratosphere during warm ENSO events. *J. Atmos. Sci.* **67**, 2331–2340 (2010).
47. E. J. Highwood, B. J. Hoskins, The tropical tropopause. *Q. J. R. Meteorol. Soc.* **124**, 1579–1604 (1998).
48. J. Keeble *et al.*, Evaluating stratospheric ozone and water vapour changes in CMIP6 models from 1850 to 2100. *Atmos. Chem. Phys.* **21**, 5015–5061 (2021).
49. S. Ho *et al.*, The COSMIC/FORMOSAT-3 radio occultation mission after 12 years: Accomplishments, remaining challenges, and potential impacts of COSMIC-2. *Bull. Am. Meteor. Soc.* **101**, E1107–E1136 (2020).
50. H. Hersbach *et al.*, Complete ERA5 from 1940: Fifth generation of ECMWF atmospheric reanalyses of the global climate (2017). Accessed 15 October 2023.
51. A. Simmons *et al.*, ERA5.1: Rerun of the Fifth generation of ECMWF atmospheric reanalyses of the global climate (2000–2006 only) (2020).
52. UCAR COSMIC Program, COSMIC-1 Data Products [Data set]. UCAR/NCAR - COSMIC. <https://doi.org/10.5065/ZD80-KD74>. Accessed 10 May 2023.
53. UCAR COSMIC Program, COSMIC-2 Data Products [Data set]. UCAR/NCAR - COSMIC. <https://doi.org/10.5065/T353-C093>. Accessed 10 May 2023.